European Journal of Medicinal Chemistry 45 (2010) 1256–1262

Contents lists available at ScienceDirect

European Journal of Medicinal Chemistry

journal homepage: http://www.elsevier.com/locate/ejmech

Short communication

Synthesis of highly functionalized barbituric acids and study of their interactions with p-glycoprotein and Mg^{2+} – Potential candidates for multi drug resistance modulation

Palwinder Singh*, Jatinder Kaur, Atul Bhardwaj

Department of Chemistry, Guru Nanak Dev University, Amritsar-143005. India

ARTICLE INFO

Article history:
Received 14 October 2009
Received in revised form
4 December 2009
Accepted 14 December 2009
Available online 22 December 2009

Keywords:
P-Glycoprotein
Multi drug resistance
Barbituric acid
Docking

ABSTRACT

A number of barbituric acids with appropriate substituent at *C*-5 position were synthesized and investigated for their interactions with p-gp and Mg^{2+}. Compounds **5**, **6**, **8**–**10**, **12**–**14** and **16** increased the basal activity of p-gp by more than 50% at 0.05 μM concentration. Molecular docking indicate a number of H-bond interactions between these molecules and the amino acid residues of ATP binding site of p-gp. These molecules also showed appreciable interactions with Mg^{2+}, an important component of efflux pump. All the results of these investigations favor the suitability of barbituric acids toward MDR modulation.

1. Introduction

Amongst the transporter proteins (ABC class of transporters) [1–3], P-glycoprotein (p-gp) [4] plays a significant role in the development of multi drug resistance (MDR) [5,6] which becomes a hurdle in the successful practice of chemotherapy of various diseases (like cancer, AIDS, tuberculosis and malaria). Two or more binding sites of p-gp (ATP binding site and drug binding site) and its flip-flop type of mechanism for the drug transportation cause a variety of substances to be transported by this protein. To get rid of drug transportation by p-gp, use of combination of chemotherapeutic agents (drug + p-gp inhibitor/substrate) seems to be the best option. P-gp inhibitors/substrates (MDR modulators [7–13]) through their interactions with this protein, either at ATP binding site or drug binding site or both the sites, avoid the efflux of drug molecules out of the cell thereby maintaining an optimum concentration of drug inside the cells. Irrespective of the untiring efforts of the scientific community, till date no MDR modulator is successfully employed for the clinical use. Since drug transportation by p-gp is supported by energy taken from ATP hydrolysis, another probable approach for MDR modulation is to cut off the energy supply to p-gp by blocking ATP hydrolysis. In addition to study the interactions of compounds directly with p-gp (at ATP and/or drug binding site), to work on the second approach for MDR modulation, chelation of Mg^{2+} from the ATP hydrolysis site could be a good option because of the pivotal role of Mg^{2+} in ATP hydrolysis [14–16]. In continuation with our programme for developing MDR modulators [17], here, compounds with a number of H-donor/acceptor sites (it is assumed that more the number of interacting sites, more is the inhibitory potency) and Mg^{2+} chelating properties are selected for investigations. Since 5-fluorouracil (an anti-cancer agent) is a substrate of p-gp, and the usefulness of barbituric acids as anti convulsant [18], anti-cancer [19] and sedative-hypnotic [20,21] agents, compounds **1**–**16** were studied for their interactions with p-gp as well as Mg^{2+}.

2. Result and discussion

2.1. Chemistry

1,3-Dimethyl-5-formyl barbituric acid was prepared by the treatment of 1,3-dimethylbarbituric acid with $CHCl_3$/KOH in ethanol/H_2O [22]. 1,3-Dimethyl-5-benzoyl/cinnamoyl barbituric acids were prepared by microwave irradiations of 1,3-dimethylbarbituric acid and benzoic anhydride/cinnamoyl chloride [23]. Stirring of a solution of 1,3-dimethyl-5-formyl/benzoyl/cinnamoyl barbituric acid and *o*-phenylene diamine/*o*-anisidine/anthranilic acid/*o*-nitroaniline/*o*-hydroxyaniline/2-aminoterephthalic acid in methanol at 35 °C provided the desirable compounds **1**–**8** (Scheme 1) [24]. Under

* Corresponding author. Tel.: +91 183 2258802 09x3495; fax: +91 183 2258819.
E-mail address: palwinder_singh_2000@yahoo.com (P. Singh).

0223-5234/$ – see front matter © 2009 Elsevier Masson SAS. All rights reserved.
doi:10.1016/j.ejmech.2009.12.033

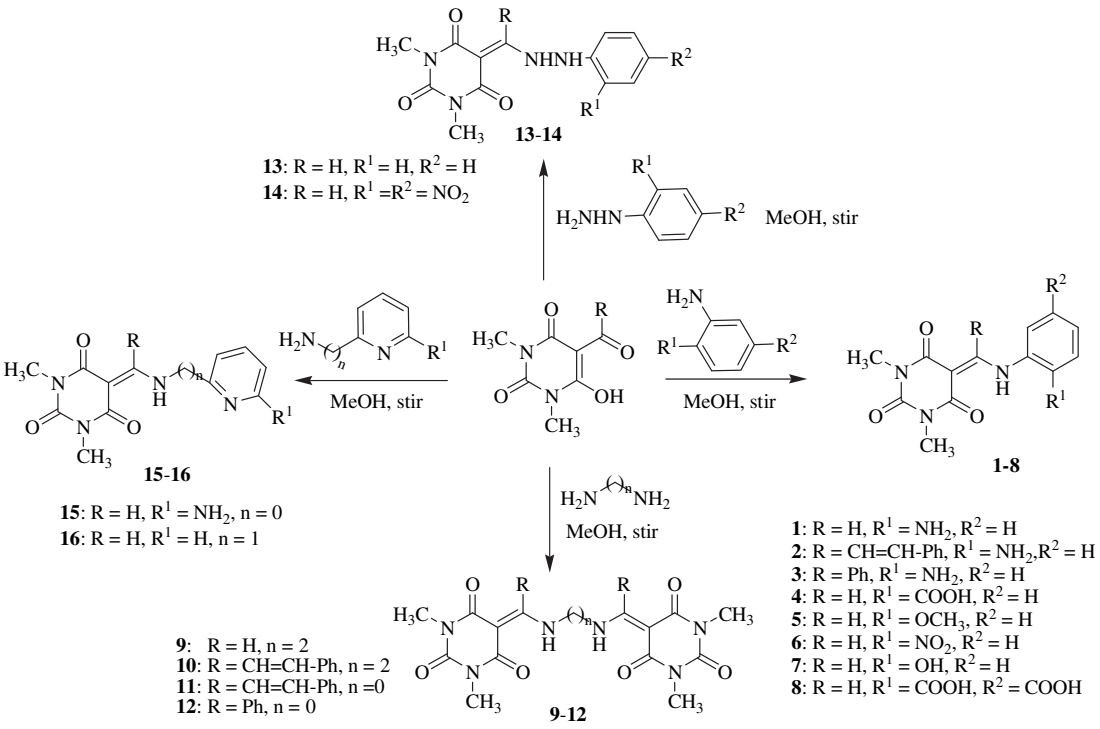

Scheme 1.

the same reaction conditions, 1,3-dimethyl-5-formyl/benzoyl/cinnamoyl barbituric acid react with hydrazine/ethylene diamine to provide compounds **9**–**12**. Similar reactions of 1,3-dimethyl-5-formyl barbituric acid with phenyl hydrazine, 2,4-dinitrophenyl hydrazine and 2,6-diaminopyridine, 2-aminomethyl pyridine gave compounds **13**, **14** and **15**, **16** respectively. Interestingly, the reactions of hydrazine and ethylene diamine with 1,3-dimethyl-5-formyl/benzoyl/cinnamoyl barbituric acids gave dimer type of products **9**–**12** but similar reactions of these barbituric acids with *o*-phenylene diamine and 2,6-diamino pyridine gave mono-substituted products **1**–**3** and **15**. Probably, this is due to the low reactivity of aromatic amines which further get decreased when one amino group gets attached to the barbituric acid moiety. The structures of all the compounds were elucidated with ^{1}H, ^{13}C NMR spectra, mass spectra and CHN analysis. Characteristically, all these compounds exist in enamine form (^{1}H NMR spectra). Therefore, following a simple synthetic procedure, a series of small organic molecules having a number of polar interacting sites were prepared.

2.2. Biology

The interactions of compounds **1**–**16** with p-gp were studied using 'Drug-P-glycoprotein Interaction' assay kit which contains the p-gp vesicles prepared from highly resistant MDR cells, the DC-3F/ADX line. The interactions of compounds with p-gp were assessed in terms of modulation of basal activity (MgATP hydrolysis activity in the absence of drug) of p-gp measured by spectrophotometric method by continuous monitoring of ADP formation in the vesicle suspension medium. The interactions of added compound (test compound) in the ATP binding site of p-gp result in the inhibition of ATPase activity of p-gp – slowing down of conversion of phosphoenolpyruvate to pyruvate and slow formation of lactate. This decreased the conversion of NADH to NAD^{+} and hence higher absorption at 340 nm (due to NADH). Therefore, the absorption of NADH at 340 nm, in the wells (96 well plate) where compound – p-gp interactions are better gets increased which was manifested as increase in the basal activity of p-gp. Compounds were tested for their interactions with p-gp at 0.05 μM, 0.5 μM and 5 μM concentrations in triplicate.

2.2.1. Interactions of compounds *1*–*16* with P-gp

As per the manufacturer's specifications for the 'drug-p-glycoprotein interactions' assay kit, on addition of a compound, a 30% change in the basal activity of p-gp implies that the compound is interacting with p-gp. All the compounds under present investigations changed the basal activity of p-gp by >30% at the three concentrations (Table 1). Amongst compounds **1**–**8**, compound **8** with two carboxyl groups present on phenyl ring exhibited best relative activity and highest increase in the basal activity (57%) of

Table 1
Relative activity and percentage increase of basal activity of p-gp by compounds **1**–**16**.

compound	Relative activity of compd (% increase of basal activity of p-gp)		
	5 μM	0.5 μM	0.05 μM
1	2.66 (166)	2.00 (102)	1.33 (33)
2	2.33(133)	2.12 (112)	1.44 (44)
3	2.35 (135)	2.44 (144)	1.42 (42)
4	2.00 (100)	1.83 (83)	1.35 (35)
5	2.23 (123)	1.95 (95)	1.53 (53)
6	2.41 (141)	1.99 (99)	1.51 (51)
7	1.95 (95)	2.14 (114)	1.42 (42)
8	2.46 (146)	1.80 (80)	1.57 (57)
9	2.34 (134)	1.71 (71)	1.66 (66)
10	1.66 (66)	2.66 (166)	2.00 (100)
11	3.00 (200)	1.69 (69)	1.33 (33)
12	2.66 (166)	2.00 (100)	1.66 (66)
13	2.68 (168)	1.97 (97)	1.57(57)
14	2.59 (159)	2.33 (133)	2.00 (100)
15	1.92 (92)	1.81 (81)	1.44 (44)
16	1.98 (98)	1.75 (75)	1.63 (63)

p-gp at 0.05 μM concentration. From this series of compounds, **5** and **6** also showed more than 50% increase in the basal activity of p-gp. In the second category of compounds i.e., **9**–**12**, compound **10** was showing maximum relative activity and highest increase in basal activity (100%) of p-gp at 0.05 μM. From compounds **13**–**14**, compound **14** with 2,4-dinitro phenyl hydrazine appendage at barbituric acid exhibited better relative activity as well as increase in basal activity (100%) at 0.05 μM in comparison to its analogue **13** indicating the additional role of nitro groups towards p-gp interactions. Compounds **15** and **16** were taken to look into any additional advantage of pyridine moiety towards MDR modulation. Although both these compounds showed appreciable increase in the basal activity of p-gp but there was no improvement over their analogues (compare **1** with **15**). Overall, compounds **5**, **6**, **8**–**10**, **12**–**14** and **16** showed more than 50% increase in the basal activity of p-gp at 0.05 μM concentration.

Therefore, it seems as these barbituric acids interact in the ATP binding site of p-gp, thereby inhibiting its ATPase activity and hence the potential candidates for p-gp mediated MDR modulation. The interactions of the compounds under present investigation in the ATP and drug binding sites of p-gp, has also been explored with molecular docking studies which indicate that these molecules show more interactions in the ATP binding site of p-gp.

2.3. Docking studies

In order to elucidate the binding modes of these molecules with p-gp, their dockings in the ATP binding site and drug binding site of this protein were performed. Compounds were built using the builder toolkit of the software package ArgusLab 4.0.1 [25] and energy minimized using semi-empirical quantum mechanical method PM3. The crystal coordinates of the p-glycoprotein (pdb ID 1MV5, pdb ID 3G60) [4] were downloaded from protein data bank. Since the drug transportation by p-gp is linked with ATP hydrolysis, blocking of ATP binding site or chelation of Mg^{2+} from this site could alter the function of p-gp. We have taken 15 $Å^3_3$ of ATP binding site in case of 1MV5 crystal coordinates and 15 Å around hexapeptide in case of 3G60 crystal coordinates, for the docking of compounds **1**–**16**. Mg^{2+} is also visible in the ATP binding site of p-gp. Validation of the docking programme was checked by docking ADP in the binding site of p-gp (Fig. 1) in which the docked ADP molecule stayed in the same binding site pocket where native ADP molecule was present. The molecule to be docked in the active site of the protein was pasted in the work space carrying the structure of the protein. The docking programme implements an efficient grid based docking algorithm which approximates an exhaustive search within the free volume of the binding site cavity. The conformational space was explored by the geometry optimization of the flexible ligand (rings are treated as rigid) in combination with the incremental construction of the ligand torsions. Thus, docking occurs between the flexible ligand parts of the compound and enzyme. The ligand orientation was determined by a shape scoring function based on Ascore and the final positions were ranked by lowest interaction energy values. H-bond and hydrophobic interactions between the compound and enzyme were explored.

Compound **1** on docking in the ATP binding site of p-gp exhibited a number of interactions with the amino acid residues. Two carbonyl oxygens of pyrimidine moiety of compound **1** show H-bond interactions with E473 and Y2393 residues. Compound **1** also interacted through its *Ns*′ (enamine nitrogen and amino nitrogen) with D468 and D2353 from a distance of 2.95 Å and 2.99 Å respectively. Remarkably, these two nitrogens, situated at a distance of 2.99 Å and 3.17 Å from Mg^{2+}, could also interact with this metal ion (Fig. 2). Docking of compound **4** (COOH group on the phenyl ring) indicate H-bond interactions between two

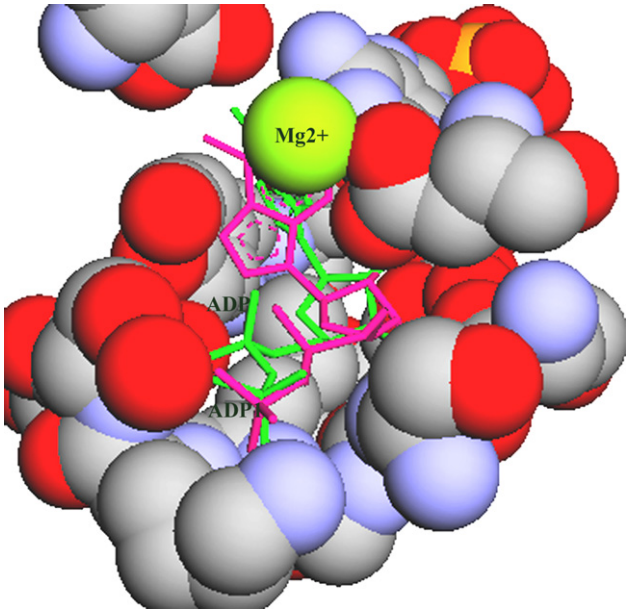

Fig. 1. Validation of docking programme. Space filled binding site of p-gp shows the presence of two ADP molecules in the pocket. ADP1 (ADP docked in the ATP binding site of p-gp, pink) is present in the same binding site pocket where the native ADP molecule (present in the crystal structure of the protein, green) was crystallized. Hs' are suppressed for clarity.

carbonyl oxygens of pyrimidine with S1383 and S1378; oxygens of carboxyl group with S2355 and G1379; enaminic *N* with D2353. One carbonyl oxygen and enaminic *N* of compound **4** are situated at a distance of 2.96 Å and 4.01 Å from Mg^{2+} (Table S1). Therefore, as per our design of the molecules and the observations from the experimental results (interactions in the ATP binding site of p-gp), docking studies also indicate the interactions of these compounds with the ATP binding site amino acids of p-gp as well as Mg^{2+}. Compounds **2** and **3** also show similar interactions with amino acid residues of p-gp but the nearest distance of any part of these compounds from Mg^{2+} is 4.0 Å.

In comparison to compounds **1**–**4**, presence of two nitrogens (in the form of hydrazine moiety) between pyrimidine and phenyl rings and an additional substituent on the phenyl ring in compound **14** makes this molecule to approach T1384 of chain B where it interacts with this residue through an H-bonding. Docking of

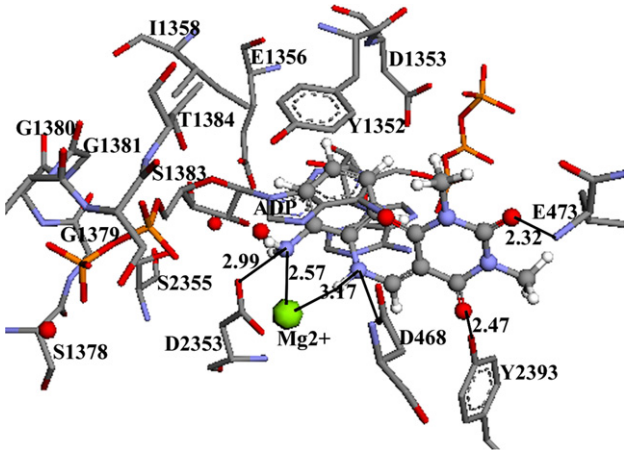

Fig. 2. Compound **1** docked in the active site of p-gp. Distances of various groups of compound **1** from the amino acid residues (within the range of H-bond interactions and electrostatic interactions) are given in Å. Hs' are omitted for clarity.

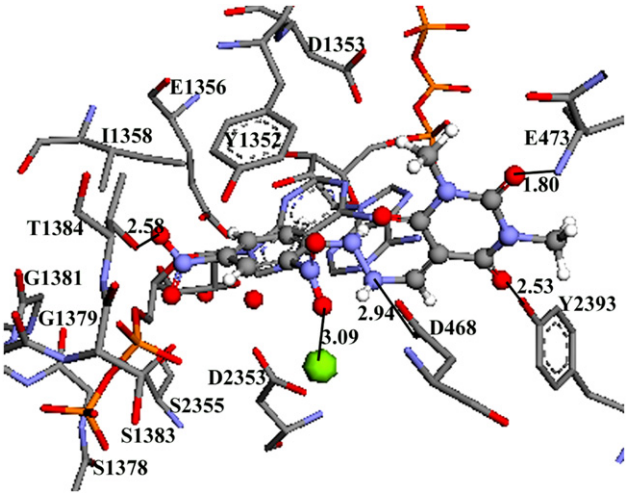

Fig. 3. Compound **14** docked in the active site of p-gp. Distances of various groups of compound **14** from the amino acid residues (within the range of H-bond interactions and electrostatic interactions) are given in Å. Hs' are ommitted for clarity.

compound **14** in the active site of p-gp indicates its interactions with E473, Y2393, D468 and T1384 amino acids present in the active site of p-gp. One of the two oxygens of C-2 nitro group approached Mg^{2+} at a distance of 3.09 Å (Fig. 3).

Symmetrical molecule **9** with an ethylene diamine moiety between two pyrimidines beautifully surrounds the Mg^{2+} where carbonyl oxygen of each of the two pyrimidines is present at a distance of 2.63 Å and 3.10 Å from Mg^{2+} (Fig. 4).

However, the replacement of methine *Hs*' of compound **9** with styryl moieties in compound **10** does not allow the molecule to approach Mg^{2+}. Docking of compound **10** in the active site of p-gp indicates its interactions with amino acid residues only. Removal of ethylene unit from compound **10**, as in compound **11**, decreases the overall volume of the molecule and docking of compound **11** (Fig. 5) in the binding site of p-gp shows its proximity to Mg^{2+} (1.33 Å) but the H-bond interactions with amino acid residues of p-gp are less in comparison to those observed for compound **10**. Compound **11** exhibits interactions with Y1352 through two carbonyl oxygens of pyrimidine moiety. Therefore, the overall volume of the molecule and the presence of interacting sites are the critical parameters in deciding its acceptability in the active site of the protein. Hence, the docking studies indicate excellent interactions of all these compounds in the ATP binding site of p-gp (Table S1).

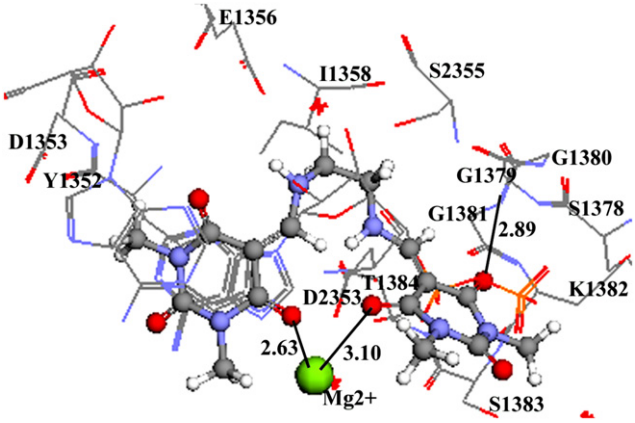

Fig. 4. Compound **9** docked in the binding site of p-gp. Chelation of Mg^{2+} by two oxygens of carbonyl groups is visible.

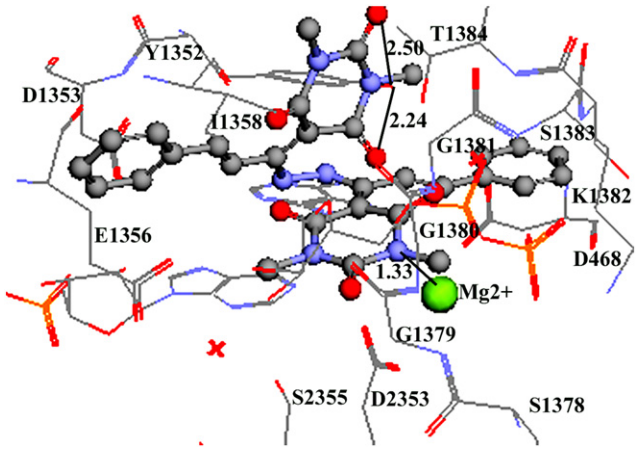

Fig. 5. Compound **11** docked in the binding site pocket of p-gp. Carbonyl oxygens of pyrimidine moiety interact through H-bonds with Y1352.

In order to make comparison between the interactions of barbituric acids in the ATP and drug binding site of p-gp, docking of these molecules were also performed in the drug binding site of p-gp using crystal coordinates of p-gp with pdb ID 3G60. These investigations indicated a single H-bond interaction of some of these molecules with the drug binding site amino acids (Table S1). As a representative, the docking of compound **1** in the drug binding site of p-gp has been shown in Fig. 6. Compound **1** showed an H-bond interaction between its carbonyl oxygen (C_2=O) and S975. Therefore, a comparison between the interactions of these barbituric acids in the ATP binding site and drug binding site of p-gp (Table S1) clearly indicated better interactions of these molecules in the ATP binding site and hence support the experimental results where a decrease in the ATPase activity of p-gp was observed.

2.4. Interactions of compounds *1–16* with Mg^{2+}

The docking studies were indicating the possibility of interactions of barbituric acids with Mg^{2+} and also the fact that

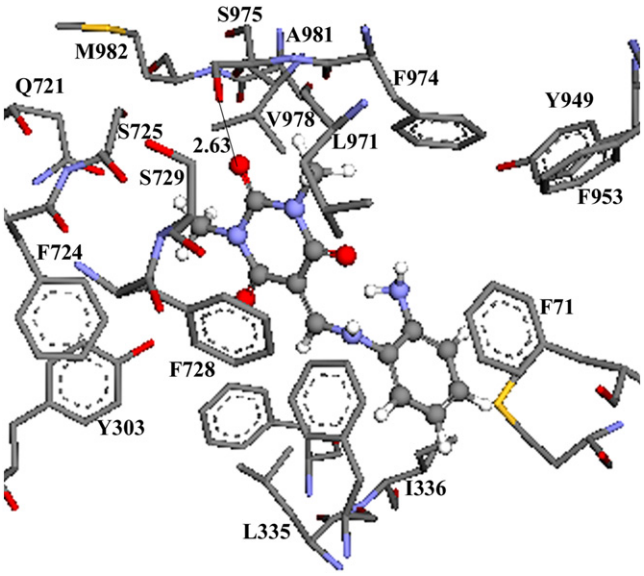

Fig. 6. Compound **1** docked in the drug binding site of p-gp. Hs' are ommitted for clarity.

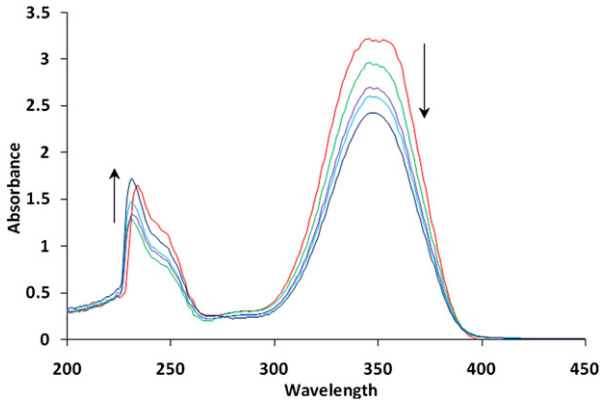

Fig. 7. Absorption spectra of compound **4** in presence of increasing concentration of Mg^{2+}(0–0.1 × 10^{-4} M). Arrows denote change in absorption with increasing concentration of Mg^{2+}.

sequestering of Mg^{2+} results in slowing down of ATP hydrolysis and hence the supply of energy to p-gp during drug effluxing, the barbituric acids under present investigations were checked for their interactions with Mg^{2+} with the help of UV-vis studies. Solutions of compounds **1**–**16** were prepared at 10^{-4} M concentrations in HEPES buffer (10^{-2} M) at pH 7.2 and titrated with Mg^{2+} solutions (0–0.1 × 10^{-4} M). All these compounds exhibit hyperchromicity in the region 230–250 nm and hypochromicity in the region 280–380 nm on addition of Mg^{2+} solution with a shift of 5 and 9 nm in case of compounds **4** and **13**. Absorption spectrum of compound **4** showing two peaks at 234 nm and 352 nm upon addition of Mg^{2+} exhibited a hypsochromic shift of 5 nm in the peak at 234 nm. Moreover, with continuous addition of Mg^{2+}, an increase in absorbance at 229 nm and a decrease in absorbance at 352 nm was observed (Fig. 7). Absorption spectra of compound **13** showing two absorption peaks at 231 nm and 300 nm, upon titration with Mg^{2+}, exhibited a continuous increase in absorbance at 231 nm with a concomitant decrease in absorbance at 300 nm (Fig. 8). There was also a hypsochromic shift of 9 nm in the 300 nm peak which gets shifted to 291 nm (Fig. 8).

The change in absorbance was plotted against mole fraction of metal ion concentration (Job plot for compound **4** and **13** is given in figure S1) to obtain the stoichiometry of Mg^{2+} - compound complexes. In all the cases, the stoichiometry of the complexes is 1:1. The association constants of Mg^{2+}-compound complexes were calculated using Benesi–Hildebrand equation [26] (Table 2). It is

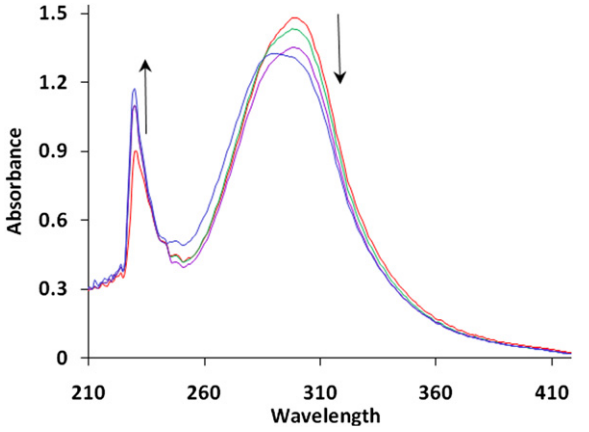

Fig. 8. Absorption spectra of compound **13** in presence of increasing concentration of Mg^{2+} (0–0.1 × 10^{-4} M). Arrows denote change in absorption with increasing concentration of Mg^{2+}.

Table 2
Association constants for Mg^{2+} binding with compounds **1**–**16** in HEPES buffer (M^{-1}).

Compd	K_a	Compd	K_a
1	7.06 × 10^5	**9**	8.68 × 10^5
2	2.7 × 10^4	**10**	5.84 × 10^5
3	2.41 × 10^4	**11**	4.82 × 10^5
4	3.6 × 10^6	**12**	1.11 × 10^6
5	5.79 × 10^5	**13**	1.53 × 10^7
6	1.40 × 10^5	**14**	1.2 × 10^6
7	5.76 × 10^5	**15**	2.57 × 10^5
8	7.46 × 10^5	**16**	3.20 × 10^5

apparent from the values of association constants that all the compounds show appreciable bindings with Mg^{2+}.

Therefore, the interactions of these compounds with Mg^{2+} could also be responsible for inhibition of ATPase activity which in consonance with the results of interactions of compounds with p-gp resulted in the modulation of p-gp activity.

3. Conclusions

The barbituric acid based compounds carrying a number of H-donor/acceptor sites were synthesized and using 'Drug–p-gp interaction assay kit', they were found to inhibit the ATPase activity of p-gp. The interactions of these molecules with Mg^{2+} also indicate the inhibition of ATPase activity in presence of these compounds. Molecular docking of these molecules in the ATP and drug binding site of p-gp showed their significantly better interactions in the ATP binding site which support the experimental results of decrease in ATPase activity by these compounds.

4. Experimental

4.1. Chemistry

Melting points were determined in capillaries and are uncorrected. ^1H and ^{13}C NMR spectra were run on JEOL 300 MHz and 75 MHz NMR spectrometer respectively using $CDCl_3$ as solvent. Chemical shifts are given in ppm with TMS as an internal reference. *J* values are given in Hertz. IR and UV spectral data were recorded on FTIR 8400S Shimadzu and BioTek PowerWave XS instruments respectively. Chromatography was performed with silica 100–200 mesh and reactions were monitored by thin layer chromatography (TLC) with silica plates coated with silica gel HF-254. In ^{13}C NMR spectral data, +ve, −ve terms correspond to CH_3, CH, CH_2 signals in DEPT-135 NMR spectra.

4.2. General procedure for synthesis of compounds *1*–*16*

The solution of 5-substituted-6-hydroxy-1,3-dimethylpyrimidin-2,4-dione and the appropriate amine (phenylene diamine/ethylene diamine/hydrazine/phenyl hydrazine/2,4-dinitrophenylhydrazine/anthranilic acid/o-anisidine/2,6-diaminopyridine/2-aminomethylpyridine/2-nitroaniline/2-aminophenol/2-aminoterephthalic acid) (1.2 equiv for compounds **1**–**8**, **13**–**16** and 0.5 equiv for compounds **9**–**12**) in methanol was stirred at 35 °C for 3–5 h. The solid suspension on filtration and washing with diethyl ether provided the pure compounds **1**–**16.** Spectral data of compounds **1**–**3** and **9**–**12** has been already reported [24].

4.2.1. 2-((Tetrahydro-1,3-dimethyl-2,4,6-trioxopyrimidin-5(6H)-ylidene)methylamino) benzoic acid (*4*)

Creamish white solid, 78% yield, mp 210 °C; ν_{max} (KBr): 1632 (C═O), 1675 (C═O), 3425 (NH), 3480 (COOH); UV λ_{max} (ε)

(DMSO + HEPES buffer) 234 (16470) and 352 (32040) nm; ^{1}H NMR ($CDCl_3$ + TFA) δ 3.39 (s, 6H, CH_3), 7.40–7.45 (t, J = 7.5 Hz, 1H, ArH), 7.68–7.70 (d, J = 8.1 Hz, 1H, ArH), 7.76–7.81 (t, J = 7.8 Hz, 1H, ArH), 8.22–8.25 (dd, J^2 = 8.1 Hz, J^3 = 1.5 Hz, 1H, ArH), 8.91–8.96 (d, J = 13.8 Hz, 1H, =CH), 13.69 (broad doublet, J = 13.2 Hz, 1H, NH); ^{13}C NMR (normal/DEPT-135) ($CDCl_3$ + TFA): δ 27.90 (+ve, CH_3), 28.72 (+ve, CH_3), 108.07 (C_5), 112.48 (+ve, ArCH), 116.25 (+ve, ArCH), 117.12 (+ve, ArCH), 120.03 (absent, ArC), 126.77 (+ve, ArCH), 136.29 (absent, ArC), 150.90 (C_2), 152.64 (+ve, CH), 160.14 (C_6/C_4), 160.71 (C_6/C_4). FAB mass m/z 304 (M^+); (Found: C 55.50, H 4.39, N 13.91; $C_{14}H_{13}N_3O_5$ requires C 55.45, H 4.32, N 13.86)

4.2.2. 5-((4-Methoxyphenylamino)methylene)-1,3-dimethylpyrimidine-2,4,6(1H,3H,5H)–trione (**5**)

Creamish white solid, 81% yield, mp 190 °C; ν_{max} (KBr): 1630 (C=O), 1650 (C=O), 3220 (NH); UV λ_{max} (ε) (DMSO + HEPES buffer) 231 (9090) and 349 (16120) nm; ^{1}H NMR ($CDCl_3$ + TFA) δ 3.36 (s, 6H, CH_3), 3.85 (s, 3H, OCH_3), 6.95–6.98 (d, J = 8.7 Hz, 2H, ArH), 7.19–7.28 (m, 2H, ArH), 8.59–8.64 (d, J = 14.1 Hz, 1H, =CH), 12.06–12.10 (broad doublet, J = 13.2 Hz, 1H, NH); ^{13}C NMR (normal/DEPT-135) ($CDCl_3$ + TFA): δ 27.24 (+ve, CH_3), 27.96 (+ve, CH_3), 55.60 (+ve, OCH_3), 92.30 (C_5), 115.21 (+ve, ArCH), 119.48 (+ve, ArCH), 131.35 (absent, ArC), 152.09 (+ve, CH), 158.35 (absent, ArC), 162.77 (C_2), 165.04 (C_6/C_4), FAB mass m/z 290 (M^+); (Found: C 58.15, H 5.22, N 14.48; $C_{14}H_{13}N_3O_5$ requires C 58.13, H 5.23, N 14.53)

4.2.3. 5-((2-Nitrophenylamino)methylene)-1,3-dimethylpyrimidine-2,4,6(1H,3H,5H)-trione (**6**)

Greenish solid, 73% yield, mp 235 °C; ν_{max} (KBr): 1635 (C=O), 1680 (C=O), 3250 (NH); UV λ_{max} (ε) (DMSO + HEPES buffer) 232 (12900) and 360 (16150) nm; ^{1}H NMR ($CDCl_3$ + TFA): δ 3.30 (s, 6H, CH_3), 6.83–6.96 (m, 2H, ArH), 7.19–7.28 (m, 2H, ArH), 8.59–8.64 (d, J = 13.9 Hz, 1H, =CH), 12.00–12.12 (broad doublet, J = 13.2 Hz, 1H, NH); FAB mass m/z 305 (M^+); (Found: 51.35, H 3.96, N 18.43; $C_{14}H_{13}N_3O_5$ requires C 51.32, H 3.98, N 18.41).

4.2.4. 5-((2-hydroxyphenylamino)methylene)-1,3-dimethylpyrimidine-2,4,6(1H,3H,5H)–trione (**7**)

Dark brown solid, 70% yield, mp 250 °C; ν_{max} (KBr): 1642 (C=O), 1665 (C=O), 3225 (NH); UV λ_{max} (ε) (DMSO + HEPES buffer) 233 (4920) and 348 (9760) nm; ^{1}H NMR ($CDCl_3$ + TFA): δ 3.35 (s, 6H, CH_3), 6.89–6.98 (m, 2H, ArH), 7.25–7.37 (m, 2H, ArH), 8.66–8.69 (d, J = 13.9 Hz, 1H, =CH), 12.45–12.47 (broad doublet, J = 13.2 Hz, 1H, NH); FAB mass m/z 276 (M^+); (Found: C 56.78, H 4.78, N 15.29; $C_{14}H_{13}N_3O_5$ requires C 56.72, H 4.76, N 15.27).

4.2.5. 2-((Tetrahydro-1,3-dimethyl-2,4,6-trioxopyrimidin-5(6H) ylidene)methylamino) benzene −1,4-dioic acid (**8**)

Creamish white solid, 75% yield, mp 255 °C; ν_{max} (KBr): 1624(C=O), 1655(C=O), 3220 (NH), 3450 (COOH); UV λ_{max} (ε) (DMSO + HEPES buffer) 232 (12990) and 350 (21240) nm; ^{1}H NMR ($CDCl_3$ + TFA): δ 3.32 (s, 6H, CH_3), 6.90–6.97 (m, 2H, ArH), 7.75–7.80 (m, 1H, ArH), 8.66–8.69 (d, J = 14.4 Hz, 1H, =CH), 13.21 (broad doublet, J = 13.7 Hz, 1H, NH); FAB mass m/z 348 (M^+); (Found: C 51.82, H 3.79, N 12.12; $C_{14}H_{13}N_3O_5$ requires C 51.88, H 3.77, N 12.10).

4.2.6. Compound **13**

White solid, 80% yield, mp 210 °C; ν_{max} (KBr): 1635 (C=O), 1680 (C=O), 3385 (NH); UV λ_{max} (ε) (DMSO + Hepes buffer) 231 (8980) and 300 (14780) nm; ^{1}H NMR ($CDCl_3$ + TFA): δ 3.27 (s, 6H, CH_3), 7.27–7.29 (d, J = 6.5 Hz, 1H, ArH), 8.29–8.31 (d, J = 7.6 Hz, 1H, ArH), 8.31–8.43 (d, J = 5.5 Hz, 1H, ArH), 8.51–8.56 (m, 2H, ArH), 8.67–8.65 (d, J = 10.7 Hz, 1H, =CH), 9.25 (broad singlet, 1H, NH), 10.16 (broad singlet, 1H, NH); FAB mass m/z 275 (M^+); (Found: C 56.95, H 5.17, N 20.46; $C_{14}H_{13}N_3O_5$ requires C 56.93, H 5.14, N 20.43)

4.2.7. 5-(N′-(2,4-Dinitrophenyl)-hydrazinomethylene)-1,3-dimethylpyrimidine-2,4,6(1H,3H, 5H)-trione (**14**)

Brownish solid, 75% yield, mp 225 °C; ν_{max} (KBr): 1635 (C=O), 1655 (C=O), 3390 (NH); λ_{max} (ε) UV (DMSO + HEPES buffer) 236 (6250) and 373 (11850) nm; ^{1}H NMR ($CDCl_3$ + TFA): δ 3.25 (s, 6H, CH_3), 7.36–7.38 (d, J = 6.6 Hz, 1H, ArH), 8.40–8.42 (d, J = 7.5 Hz, 1H, ArH), 8.50–8.52 (d, J = 5.7 Hz, 1H, ArH), 8.61–8.65 (d, J = 10.8 Hz, 1H, =CH), 9.18 (broad singlet, 1H, NH), 10.23 (broad singlet, 1H, NH); ^{13}C NMR (normal/DEPT-135) ($CDCl_3$ + TFA): δ 28.25 (+ve, CH_3), 28.98 (+ve, CH_3), 108.74 (C_5), 112.51 (+ve, ArCH), 114.90 (+ve, ArCH), 116.27 (+ve, ArCH), 123.88 (absent, ArC), 131.07 (absent, ArC), 140.21 (absent, ArC), 146.44 (C_2), 161.61 (+ve, CH), 162.76 (C_6/C_4), 163.04 (C_6/C_4). FAB mass m/z 365 (M^+); (Found C 42.89, H 3.38, N 23.10; $C_{14}H_{13}N_3O_5$ requires C 42.86, H 3.32, N 23.07).

4.2.8. 5-(((6-Aminopyridine-2-yl)methylamino)methylene)-1,3-dimethylpyrimidine-2,4,6(1H, 3H,5H)-trione (**15**)

Brownish solid, 72% yield, mp 240 °C; ν_{max} (KBr): 1632 (C=O), 1675 (C=O), 3258 (NH); UV λ_{max} (ε) (DMSO + HEPES buffer) 237 (10920), 280 (14040) and 362 (6050) nm; ^{1}H NMR ($CDCl_3$ + TFA): δ 3.38 (s, 6H, CH_3), 4.00 (s, 2H, NH_2), 6.10–6.19 (m, 2H, ArH), 7.28–7.35 (m, 1H, ArH), 7.66–7.68 (d, J = 13.9 Hz, 1H, =CH), 12.25–12.29 (broad doublet, J = 13.2 Hz, 1H, NH); FAB mass m/z 276 (M^+); (Found: C 52.32, H 4.75, N 25.48; $C_{14}H_{13}N_3O_5$ requires C 52.36, H 4.76, N 25.44).

4.2.9. 5-(((Pyridine-2-yl)methylamino)methylene)-1,3-dimethylpyrimidine-2,4,6(1H,3H,5H)-trione (**16**)

Brownish solid, 70% yield, mp 170 °C; ν_{max} (KBr): 1645 (C=O), 1687 (C=O), 3236 (NH); UV λ_{max} (ε) (DMSO + HEPES buffer) 238 (11190), 282 (14310) and 360 (7030) nm; ^{1}H NMR ($CDCl_3$ + TFA): δ 3.38 (s, 6H, CH_3), 4.12 (s, 2H, CH_2), 6.90–6.98 (m, 2H, ArH), 7.85–7.95 (m, 2H, ArH), 8.66–8.69 (d, J = 13.9 Hz, 1H, =CH), 12.35–12.38 (broad, 1H, NH); FAB mass m/z 275 (M^+); (Found: C 56.92, H 5.17, N 20.45; $C_{14}H_{13}N_3O_5$ requires C 56.93, H 5.14, N 20.43).

4.2.10. p-gp interaction studies

Solutions of compounds **1**–**16** which are tested for their interactions with p-gp were primarily prepared at 10^{-2} M concentration and diluted to three concentrations 0.5 μM, 5 μM and 50 μM. Further dilutions take place during the assay and the final concentrations become 0.05 μM, 0.5 μM and 5 μM. Each well of 96 well plate was dispensed with 80 μL of enzymatic buffer, 20 μL of PK/LDH solution, 10 μL of PEP solution and 10 μL of NADH solution. Additionally, 60 μL of enzymatic buffer was added to the total activity well; 30 μL of non-specific ATPase inhibitor solution and 30 μL enzymatic buffer was added to basal activity well and 30 μL non-specific ATPase inhibitor solution, 30 μL enzymatic buffer to non-specific activity well. Blank well contains 200 μL of enzymatic buffer. The plate was incubated for 30 min at 37 °C. 10 μL of enzymatic buffer was added to non-specific activity wells and 10 μL of membrane vesicles were added to all other wells except blank well. Plate was incubated for 5 min at 37 °C, dispensed 20 μL of compound at each concentration and again incubated for 5 min at 37 °C. Finally, 10 μL of MgATP was added to each well except blank well and plate was incubated for 20 min at 37 °C. Plate was read at 340 nm followed by incubation and again reading (after 20 min).

4.3. Mg^{2+} binding studies

Stock solutions (10^{-2} M) of compounds **1**–**16** were prepared by dissolving the compounds in 2–3 drops of DMSO and diluting with HEPES buffer (10^{-2} M) at pH 7.2. The complex formation was studied by incremental addition of metal ion to 10 μl of ligand solution making final volume 1 ml. The binding constants of

compounds **1**–**16** with Mg^{2+} were calculated using Benesi Hildebrand Equation (supplementary information).

4.4. Docking procedure

Compounds were built using the builder toolkit of the software package ArgusLab 4.0.1 and energy minimized using semi-empirical quantum mechanical method PM3. The crystal coordinates of the p-glycoprotein (pdb ID 1MV5, pdb ID 3G60) were downloaded from protein data bank and in the molecule tree view of the software, the monomeric structure of the crystal coordinate was selected and the active site was defined as 15 Å around the ligand. In the workspace, carrying the structure of protein, the structure of the molecule to be docked was pasted. Then the docking experiment was performed during which molecule get docked in the active site of protein and places itself in its most favorable orientation. The docking was repeated several times (approx. 10000 iterations) until no change in the position of the ligand and a constant value of the binding energy was observed.

Acknowledgements

Financial assistance from DST, New Delhi is gratefully acknowledged. JK thanks UGC and AB thanks DST for fellowships. Department of Applied Chemistry, GNDU, Amritsar is acknowledged for recording IR spectra and CDRI, Lucknow is acknowledged for recording mass spectra.

Appendix. Supplementary data

Supplementary data associated with this article can be found in the online version at doi:10.1016/j.ejmech.2009.12.033.

References

[1] H.W.V. Veen, C.F. Higgins, W.N. Konings, Res. Microbiol. 152 (2001) 365–374.
[2] P.D.W. Eckford, F.J. Sharom, Chem. Rev. 109 (2009) 2989–3011.
[3] J.-P. Gillet, T. Efferth, J. Remacle, Biochim. Biophys. Acta 1775 (2007) 237–262.
[4] S.G. Aller, J. Yu, A. Ward, Y. Weng, S. Chittaboina, R. Zhuo, P.M. Harrell, Y.T. Trinh, Q. Zhang, I.L. Urbatsch, G. Chang, Science 323 (2009) 1718–1722.
[5] E. Teodori, S. Dei, S. Scapecchi, F. Gualtieri, Il Farmaco 57 (2002) 385–415.
[6] A.H. Dantzig, K.L. Law, J. Cao, J.J. Starling, Curr. Med. Chem. 8 (2001) 39–50.
[7] G. Szakacs, J.K. Paterson, J.A. Ludwig, C. Booth-Genthe, M.M. Gottesman, Nat. Rev. Drug Discov. 1 (2006) 585–594.
[8] T.J. Raub, Mol. Pharmaceut 3 (2006) 3–25 and references therein.
[9] M. Kawase, N. Motohashi, Curr. Drug Targets 4 (2003) 31–43.
[10] E.-M. Collnot, C. Baldes, M.F. Wempe, R. Kappl, J. Huttermann, J.A. Hyatt, K.J. Edger, U.F. Schaefer, C.-M. Lehr, Mol. Pharmaceut 4 (2007) 465–474.
[11] X.-L. Liu, H.-W. Tee, M.-L. Go, Bioorg. Med. Chem. 16 (2008) 171–180.
[12] N.A. Colabufo, F. Berardi, M. Cantore, M.G. Perrone, M. Contino, C. Inglese, M. Niso, R. Perrone, A. Azzariti, G.M. Simone, L. Porcelli, A. Paradiso, Bioorg. Med. Chem. 16 (2008) 362–373.
[13] M.K. Gannon, J.J. Holt, S.M. Bennett, B.R. Wetzel, T.W. Loo, M.C. Barlett, D.M. Clarke, G.A. Sawada, J.W. Higgins, G. Tombline, T.J. Raub, M.R. Detty, J. Med. Chem. 52 (2009) 3328–3341.
[14] A.L. Lehninger, D.L. Nelson, M.M. Cox, Principles of Biochemistry CBS, second ed. (1992), ISBN 81-239-0295-6 p374.
[15] A. Gomez-Puyou, G. Ayala, U. Muller, T. de. Gomez-Puyou, J. Biol. Chem. 258 (1983) 13673–13679.
[16] R.C. Phillips, P.S.J. George, R.J. Rutman, J. Am. Chem. Soc. 88 (1966) 2631–2640.
[17] P. Singh, J. Kaur, P. Kaur, S. Kaur, Bioorg. Med. Chem. 17 (2009) 2423–2427.
[18] L.S. Goodman, A. Gilman, The Pharmacological Basis of Therapeutics. McGraw-Hill, New Delhi, (1991), 358–360.
[19] D.J. Guerin, D. Mazeas, M.S. Manoj, F.N.M. Naguib, O.N.A. Safarjalani, M.H. Kauni, R.P. Panzica, Bioorg. Med. Chem. Lett. 9 (1999) 1477–1480 (and references therein).
[20] G. Andrews, Medical Pharmacology, The CV Mosby Company, Saint Louis, (1976), 243.
[21] W.O. Foye, Principles of Medicinal Chemistry, Lea & Febiger, London, (1989), 159.
[22] B.S. Jursic, D.M. Neumann, Tetrahedron Lett. 42 (2001) 8435–8439.
[23] P. Singh, K. Paul, Ind. J. Chem. 44B (2005) 1105–1108.
[24] P. Singh, J. Kaur, K. Paul, Ind. J. Chem. 47B (2008) 291–296.
[25] ArgusLab, M.A. Thompson, Planaria Software LLC, Seattle, WA 98155.
[26] J.H. Hildebrand, H.A. Benesi, J. Am. Chem. Soc. 71 (1949) 2703–2707.